Available online at www.CivileJournal.org

Civil Engineering Journal

(E-ISSN: 2476-3055; ISSN: 2676-6957)

Vol. 7, No. 05, May, 2021

Review Article

Experimental Studies and Analysis on Mobilization of the Cohesionless Sediments Through Alluvial Channel: A Review

Akash Anand [1*], Mubeen Beg [2], Neeraj Kumar [3]

[1] *Research Scholar, Civil Engineering Department, Aligarh Muslim University, Aligarh, India.*

[2] *Professor, Civil Engineering Department, Aligarh Muslim University, Aligarh, India.*

[3] *Research Scholar, Civil Engineering Department, Sam Higginbottom University of Agriculture, Technology and Sciences, Allahabad, India.*

Received 14 January 2021; Revised 26 March 2021; Accepted 11 April 2021; Published 01 May 2021

Abstract

Entrainment of river bed particles by turbulent flow is a core matter of study in river hydrodynamics. It is of great interest to river engineers to evaluate the shear stress for initiating river bed motion. The main objective is to calculate transport rates for bed load, to predict changes in bed level which are scoured or aggraded and to design a stable channel. Forces acting upon the particle especially fluid forces which give a major role in the incipient motion of the particle on the rough boundary. For calculation generally use shield's diagram but some other modified methods and approaches are discussed. Modeling criteria are discussed for the hydraulically smooth and rough boundary depending on Reynolds number. In the past, experimental studies on tractive shear stress have been done by many researchers but consideration of lift force to analyze the movement of sediment is very limited. For suspended load transport, a detailed analysis of lift force is required. Based on the study it has been observed that shear stress depends on channel slope not only due to gravitational force but also many other factors like drag force, lift force, friction angle, fluctuations, velocity profile, etc. Complete analysis of these factors provides slope dependency over shear stress. To improve past studies, some factors have been discussed, to give a more correct force balance equation. This is very difficult task to analyze more and more variable's dependency on the slope. Consideration of the possible number of variable holds complete analysis of experimental study. This paper also reviews the effect of particle Reynolds number and relative submergence over critical shield stress.

Keywords: Tractive Shear Stress; Turbulent Flow; Shield's Diagram; Incipient Motion; Local Velocity; Particle Reynolds Number.

1. Introduction

There is the most important problem in the transport mechanism of the sediment is the estimation of the flow intensity at which the movement of the sediment starts. This movement of the grain particles is achieved at a critical level where shear stress is such that it will start the motion. This shear is called critical tractive bed shear stress. It either minimum shear stress responsible for the motion of the grains or bigger size of the grain that comes in motion for a particular value of given shear stress. Forces on bed particle: If the average tractive bed shear stress is not able to move the bed particles, the grains or river bed will be on rest. Hence it doesn't accelerate the river bed because all resultant force on it must be in balance [1-3]. There are 3 main types of forces acting on the particle:

* Corresponding author: aanand@myamu.ac.in

http://dx.doi.org/10.28991/cej-2021-03091700

© 2021 by the authors. Licensee C.E.J, Tehran, Iran. This article is an open access article distributed under the terms and conditions of the Creative Commons Attribution (CC-BY) license (http://creativecommons.org/licenses/by/4.0/).

I. Submerged weight of the particle: It is simply a total downward weight of particle minus upward buoyant force. It acts as center of mass of the particle also known as an effective weight of the particle.

II. Force of contact between two particles: This force acts when one particle rest on another particle and through action- reaction law both particles will have a force of contact.

III. Forces due to fluid motion acting on the particle: The fluid forces are much harder to manage. They need sufficient information on the dynamics of flow that is very close to the bed. This flow is shear flow with turbulence [4, 5].

During the analysis of sediment motion, a deal with the local flow (local flow velocity, local flow pressure) around the particle is considered and this flow is turbulent. Due to fluid flow, frictional shear stress (viscous shear drag) and pressure force (form drag) act upon the particle (Figure 1).The Equilibrium of all forces decides the movement of a particle. Drag forces and lift forces are the forces due to flowing fluid act upon the particle and responsible for the motion of the particle. The resulting force varies greatly with time, from tiny fractions of a second to several minutes. This phenomenon is valid Even if the time-averaged flow is steady or though the particle is inside the viscous sublayer [6, 7].

τ_o is a good indicator of the movement of the bed particle at the threshold condition, as it represents the mean force on the bed particles. However, this assertion has an important attribute in that planner bed. And this planner bed should not have any landform or else most of the part of total tractive bed shear stress will spend in form drag (pressure drag).But for particle motion, viscous shear stress plays a major role to drive the particles. Here resisting forces are the submerged weight of particle and contact forces. The submerged weight acts a moment in an anticlockwise direction called stabilization moment [8, 9]. The moment has been taken from a pivoted point. The Resultant fluid force applies a moment in a clockwise direction called destabilization moment. Entrainment of the particle will be sliding, rolling, or lifting according to the resulting force condition (Figure 2).

For a small value of Re* shown in Figure 3(a) (which leads the particle Reynolds number based on the local flow velocity around the particle) the upper portion of the particle does not have a clearly defined boundary layer so there is no flow separation holds behind the sediment particle. For this case, both forces due to viscous and pressure are essential. The action line of the resulting force lies well above the particle's center of mass since its viscous force is greatest on the top surface. Figure 3(b) also shows line of action of total force due to fluid exists well above particle's centers of gravity point and also shows a viscous force is greatest on the top surface [6, 9, 10].

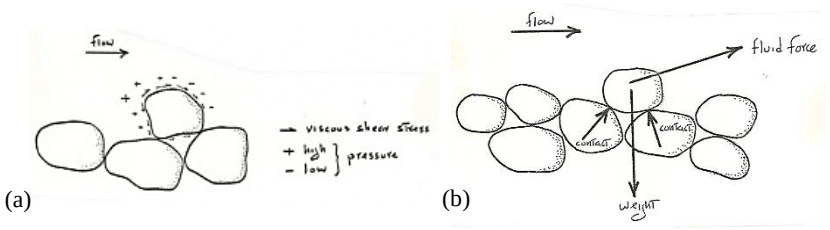

Figure 1. All three forces acting on a bed of sediment particles resting on one above [6]

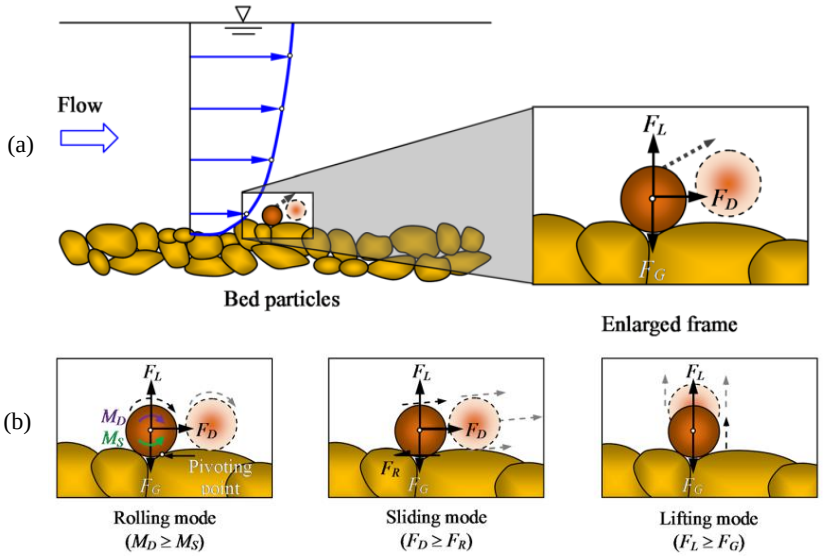

Figure 2. Mobilization of the sediment particles through fluctuation of turbulence near the bed [12] (a) Movement of the sediment grain shown by dotted line; (b) Threshold condition for particle depends on the equilibrium of major forces that generates rolling and sliding on bed and lifting on the water as a suspended load.

For a large value of Re* shown in Figure 3(b) (which leads the particle Reynolds number based on the local flow velocity around the particle) there is the destruction of viscous sublayer and here form drag is greater than skin friction. At this stage, particle Reynolds number becomes nearly independent of critical tractive shield stress. Pressure forces or form drag greatly dominate viscous skin forces. Due to the pressure difference from the front portion of a particle to the back portion, the resulting force's line of action is closer to the particle's center of mass [6, 11].

High pressure exists at the bottom portion of the particle and low pressure at the top and it follows the Bernoulli principle. It gives the idea of the force of lifting at the particle. The lift force becomes nearly equivalent to the form drag at high particle Reynolds numbers. According to experimental data, it is obvious that the lifting force generally becomes feebly negative at very low Reynolds [5, 7].

Fluid forces are extremely unsteady due to fluctuation in velocity profile associated with large wakes. Actual measurements have shown fluctuations in the instantaneous fluid forces on bed particles. A lift force on the sediment particle is acted due to high pressure around the base of the particle and low at the top surface of the particle. Researchers have made few experiments to measure the lift force and it is found that the lift force is equal to drag force at a high value of Reynolds number [9].

When the resultant forces due to drag (form and viscous) and lift become sufficiently large such that they can neutralize the effect of forces due to gravity and contact frictional resistance then at this condition, the particle will come into a state of motion. The Moment balance equation for all sediment particles cannot be explained individually because the location of some particles will be such that they can slide, lift, or roll very easily. There are some basic equations to explain the general entrainment motion of the particle [12, 13].

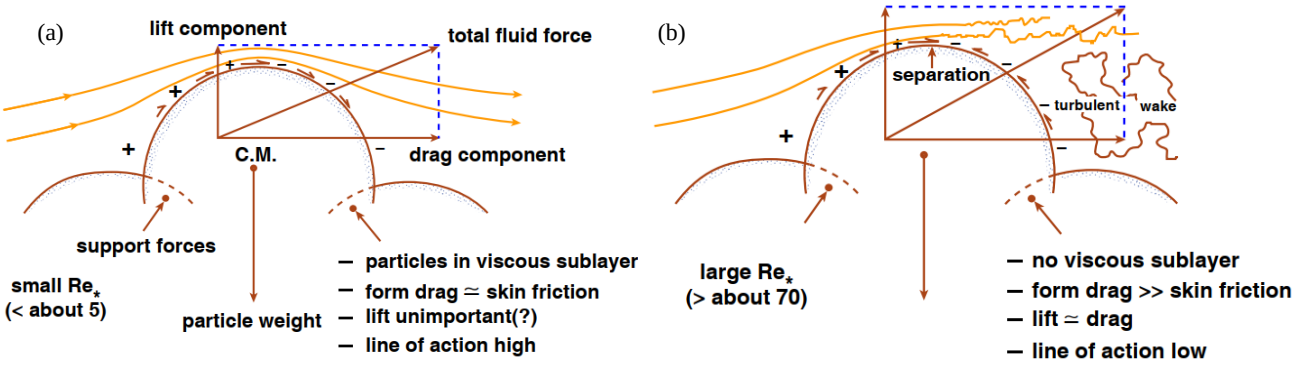

Figure 3. Total resultant Forces at different particle Reynolds number (a) Low value of particle Reynolds number; (b) High value of particle Reynolds number [6]

$$M_D \geq M_S \rightarrow F_D l_v + F_L l_h \geq F_G l_h \quad (1)$$

$$F_D \geq F_R \rightarrow F_D \geq K_{fr}\left(F_G - F_L\right) \quad (2)$$

$$F_L \geq F_G \quad (3)$$

M_D is moment due to force component of drag and lifts from the pivoted point;

M_S is the moment due to the force component of gravity from the pivoted point;

F_L is the force due to lifting acting upward, F_G is the force due to gravity acting downward;

F_R is frictional resistance between the sediment particles;

l_h is lever arm responsible to give a moment for the component of lift force;

l_v is lever arm responsible to give a moment for a component of drag force;

K_{fr} is tanϕ where ϕ is the angle of internal friction.

1.1. Different Approaches on Particle Motion and Shields Diagram

There are three methods widely used named critical velocity concept, lift force concept, Threshold, or critical tractive shear stress concept to find the entrainment condition. Critical tractive shear stress is widely used and most acceptable for certain ranges of particles. One question arrives why researchers go for critical shear stress not for the force or velocity concept generally. So right explanation is it is connected with Reynolds number (high and low) and it decides the force to act on the individual particle. This time-averaged force per unit area provide average shear stress (time-averaged) into the particle. If this average shear stress is greater than tractive shear stresses, the particle will dislocate from the position. Whatever velocity or forces are mentioned, they are local forces or local velocity acting on the particle [12, 14, 15].

Shields (1936) was the researcher who experimented upon this analysis shown in Figure 4(a). He plotted the graph between the boundary shield parameter and boundary Reynolds number. To more understanding the data collection, he did his experiments in 0.8m length and 0.4 m wide flumes. Beds were composed of granite material with diameter range (0.85 to 2.4 mm), coal with specific gravity of 1.27 g/cm^3 and diameter range 1.8 to 2.5 mm, amber with specific gravity 1.06 g/cm^3 with diameter value 1.6 mm, and barite with specific gravity 4.2 g/cm^3 with diameter range (0.36 to 3.4 mm). He finds total shear stress on the bed through the resistance equation. For each run bed level was done plane. It means for each run there is a different discharge and mean velocity value, and the slope was altered to maintain uniform flow. Through this process, grains move on the bed and finally, these bed load was collected in a trap fixed downward of the flume. And now he had a total rate of sediment transport for a given discharge. This process was done for different grain bed particles for different discharge values. The movement of the grain was not determined with direct observation. He extrapolated the value of shear stress at which no collection of sediment at trap means zero rates of transport. And due to this, a small modification was done by a miller called the modified shield curve. The shield had no data for Reynolds no less than 6 and greater than 600, and in between Reynolds number's range decides the flow regime which will be whether hydraulically smooth or rough flow regime. If the boundary Reynolds number is less or equal to 2 it shows a smooth regime. Shields had very little data in this range so he extrapolated the threshold value of shear stress. If this is greater than 2 and up to 600 then it shows a rough regime [6, 16]. Boundary Reynolds number and boundary shield parameter both are non-dimensional numbers and threshold value depends upon relative density, dynamic viscosity, grain diameter, Reynolds number shown in Equation 4. Dimensional analysis (Rayleigh's method and Buckingham method) can be done between shield parameter and Reynolds number [90].

$$\text{Threshold value} = f(\rho, \rho_s, \mu, \gamma' D, \tau_o) \tag{4}$$

Boundary shield parameter is a function of Reynolds number and relative density of the sediment shown in Equation 5:

$$\frac{\tau_c}{\gamma' D} = f\left(\frac{\rho u_* D}{\mu}, \frac{\rho_s}{\rho}\right) \tag{5}$$

Miller et al. (1977) plot is also used very much shown in Figure 4(b). Buffington and Montgomery (1997) plot is a very recent diagram to the analysis of threshold value [7, 17]. They noticed a significant change in the positioning of the Shields curve. Shields plot is log-log plot based on sediment bed load transport rate. But Buffington and Montgomery plot is based upon 'watch the bed' method. Results of shields method for critical tractive stress are more than Buffington and Montgomery plot (Figures 4c and 4d).

(a)

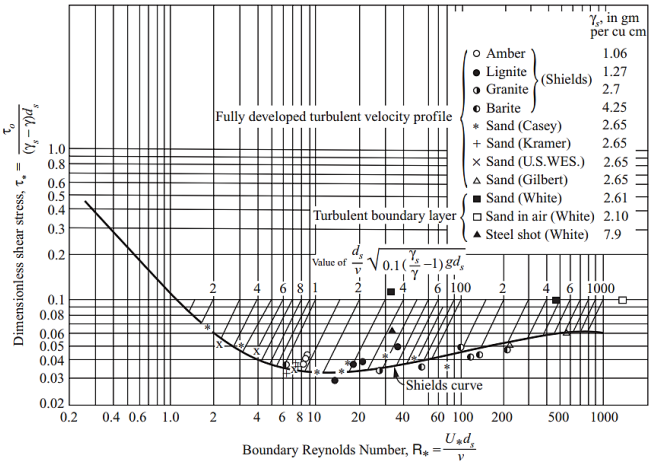

(b)

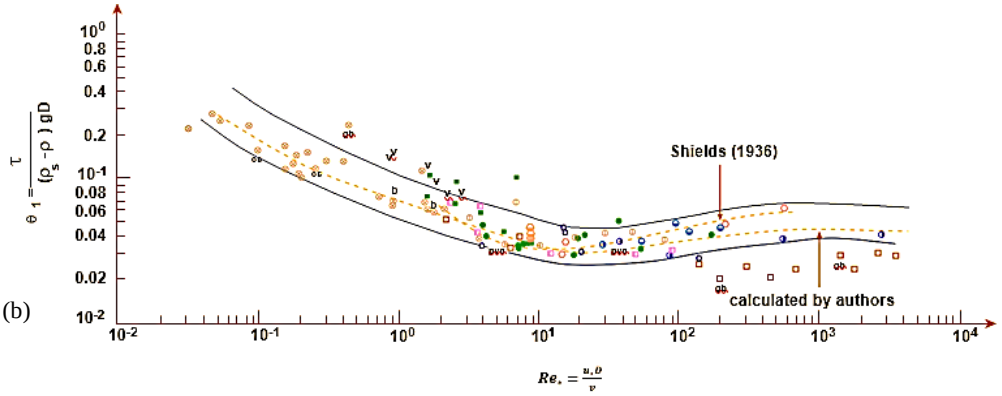

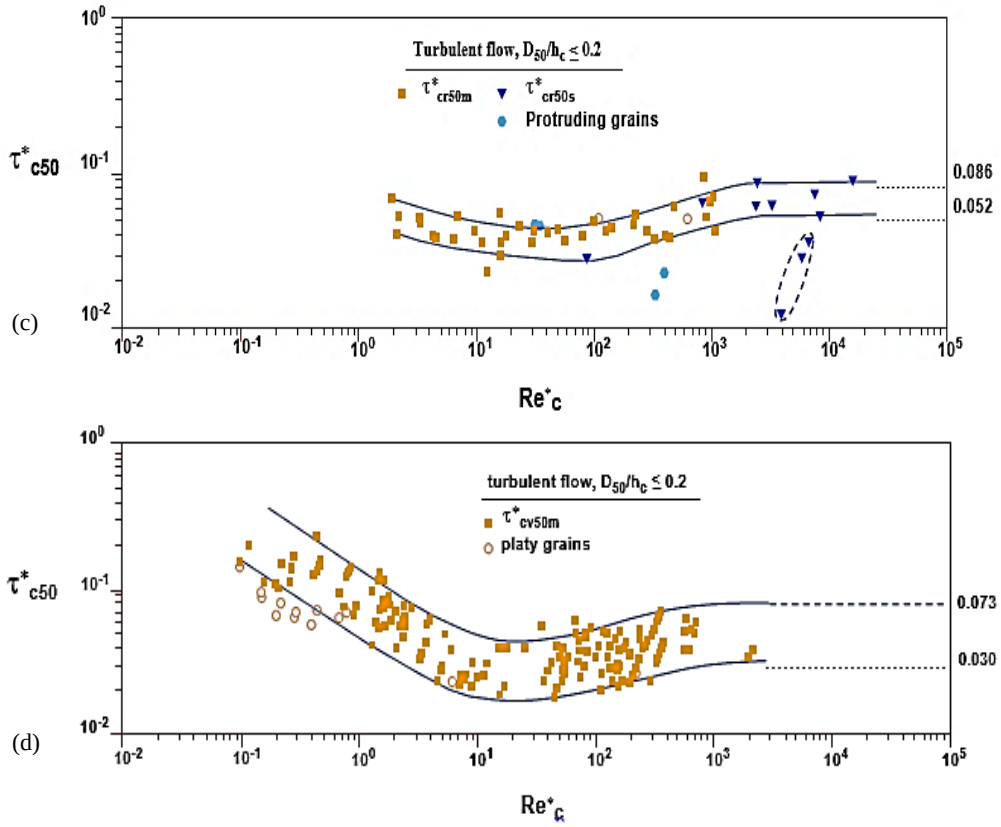

Figure 4. Graph between shield parameter and Reynolds number (a) From shield [89]; (b) From Miller et al, 1977 [7]; (c), (d) Comparison between shield and Buffington and Montgomery (1997) [17]

In many studies, the possibility of the effect of sediment density relative to water is given very less. Shields diagram shows very less effect of relative density for different particles [18, 19]. Nevertheless, many authors' studies show sufficient effect of relative density of sediments. Particles, having greater density means greater mass (inertia) relative to water, does not move during sudden change of force. There is a high value of threshold needed to start the motion. If shield parameter shows any reduction with increasing value of density ratio, then it should be the case of particles under winds. Quartz particles shows this effect [20, 21]. Shields gave many ideas to the researchers to model the bed threshold shear concept based on different mechanics on sediment particles. These are called different approaches on particle entrainment motion. These are the deterministic approaches [22].

I. White's approach: In this approach, whites considered the sliding motion of particles during threshold. He ignored the lift force in force balance equation so entrainment motion will be only due to drag force. He also determined the hydraulically smooth flow regime at Reynolds number less than 3.5 where only frictional drag will act and there will be the absence of pressure or form drag hence flow will be smooth. He found shield parameter value for this range 0.095 [23].

For transitional and rough flow regimes, Reynolds number will be greater than or equal to 3.5.Here normal drag or form drag will act in major and very less effect of viscous hence flow on the bed will be rough. He found shield parameter value for this range 0.044.

II. Kurihara's approach: Analysis of White's approach further oriented by Kurihara. He derived an expression for the turbulence factor (T_f). He gave some empirical equations to find the value of the boundary shield parameter. This factor is a function of the intensity of turbulence, boundary Reynolds number (R*), and probability to increase the tractive shear stress of the bed [24].

III. Iwagaki's approach: He provided detailed information of the force to entrainment motion of particles. He divided the force of drag into force of viscous (skin friction) drag (F_{D_v}) and turbulence drag force (F_{Dt}) means a particle having viscous sub layer and turbulence layer [25]. It is shown in Equations 6 and 7 respectively.

$$F_{Dv} = \frac{1}{2} C_{Dv} \frac{\pi}{4} d^2 (1-\beta_t) \rho f \bar{u}^2_{\delta v} \tag{6}$$

$$F_{Dt} = \frac{1}{2} C_{Dv} \frac{\pi}{4} d^2 \beta_t \rho f \bar{u}^2_{d} - \frac{\pi}{4} d^2 \beta_t d \left(\frac{\partial p}{\partial x} \right) \tag{7}$$

Igwagki divided the flow regime into three-part based on the value of boundary Reynolds number. If $R^*<6.83$ then flow will be hydraulically smooth and targeted particles will be on laminar sublayer. If $R^*\geq 51.1$ then flow will be hydraulically rough and the targeted particles will be on turbulent flow and bed roughness destroys the viscous sub layer. If $6.83 < R^* < 51.1$ then flow will be transitional regime it means both viscous sub layer and turbulent layer will exist on targeted particles.

IV. Wiberg and Smith's approach: In this approach Sliding mode of the particle is used to calculate critical shear stress. He derived lift force in terms of the difference of the square of velocities at the upper and bottom portion of the target sediment particles. He used different velocity profiles for hydraulically smooth and rough flow regimes. For a rough regime, he used a logarithmic velocity profile [26, 27].

V. Dey'sapproach: He derived threshold condition for three-dimensional compact dense bed configuration. He considered the analysis for the rolling mode of particles. Dey splits the flow regime into three-part based on the value of boundary Reynolds number. If $R^*\leq 3$ then flow will be hydraulically smooth and velocity distribution follow the linear law of velocity. If $R^*>70$ then flow will be hydraulically rough and velocity distribution follow logarithmic law of velocity. If $3 < R^* < 70$ then flow will be transitional regime and velocity distribution follow Reichardt's velocity distribution [16, 28].

From the studies on many literature reviews, authors provided very less consideration of density ratio to threshold the motion of grains even shield also took slight effect on density ratio based on their data to plot the shield diagram. Later Ward also provided the same effect on density ratio but for a larger range of difference in shield parameter. The decrease in dimensionless shear parameter with increasing the value of density ratio looks obvious. Wind tunnel theory of threshold (Mars Wind tunnel theory and Venus Wind tunnel theory) should be modified in the future.

1.2. Objective

This paper reviews the dependency of slope upon threshold shear stress and slope of the alluvial channel depends upon drag due to wall, morphological effect, friction angle, average flow velocity, drag and lift coefficient, air entrainment, relative submergence, etc. There is more work required to check channel slope dependency with other variables. These variables provide the behavioral stage for critical shield stress with respect to slope. A little contribution has been shown to make slope study more effective. This review study aims to understand the past experimental analysis (made by many researchers) of different sizes and shape of cohessionless particles (sand and gravel) over bed slope of the channel. Flume data and field data are compiled to check the natural tendency of critical stress over bed slope. Experimental analysis of different variables like particle Reynolds number, velocity profile at different layer bed, relative roughness, relative submergence etc. also has been reviewed through the graph.

2. Research Methodology

The Study of many researchers has been reviewed through a flow chart in Figure 5. Some researchers performed only experimental analysis but some others verified with field data to achieve proper validation of the analysis. The performance and results of flume and field analysis go very similar. That's why in the past, researchers have done major works related to sediment transportation in the flume due to ease of analysis.

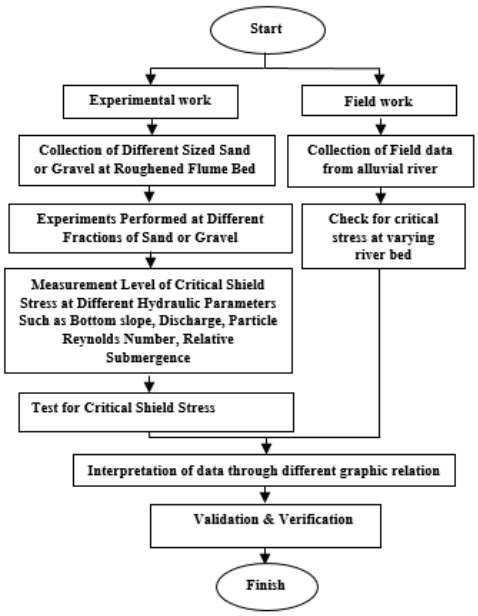

Figure 5. Flowchart of the research methodology

According to some standard model or theoretical observation when slope of the channel bed increases it can be considered that it causes instability for bed particles due to addition of downstream force of gravity. But according to the literature review and experiments made on the flume and Natural River or any stream for slope dependency, it has been observed that shield stress increases while increasing the slope of the bed. This phenomenon shows that particles are more stable at high or steeper slopes. So theoretical and experimental data observation are contrary to each other with respect to slope dependency.

This disparity may be explained by some simple models like force balancing with the slope for critical shield stress. Here through this analysis, Lamb et al. (2008) [29] observed slope dependency on drag forces, friction angles, grain emergence, flow velocity, flow aeration, and fluctuations through turbulent or eddies. But they observed that changes in drag force do not depend on the slope. The angle of internal friction, angle of repose, emergence of the grain from the flow, flow velocity, flow aeration to decrease the density of the flow and fluctuations depend upon normal to a steeper slope. Due to slope variation relative roughness (ratio of the roughness of bed to flow depth) will increase [29, 30].

The shields stress is defined as:

$$\tau_{cg}^{*} = \frac{\tau_g}{(\rho_s - \rho) gD} = \frac{u_*^2}{rgD} \tag{8}$$

$$r = \frac{\rho_s - \rho}{\rho} \tag{9}$$

$$u_* = \sqrt{\frac{\tau_g}{\rho}} \tag{10}$$

$$\mathrm{Re}^* = \frac{u_* D}{\upsilon} \tag{11}$$

τ_g=Total tractive bed shear stress (form drag+viscous shear stress) (g subscript denotes part of total bed stress acting on grains on the bed;

u_*^2 =Shear velocity;

D=Diameter of the particle;

r=Submerged specific density of the particle;

Re^* =Particle Reynolds number.

If particle Reynolds number is greater than 100 means diameter more than 3mm (in case of rivers) then shield stress will roughly constant the value 0.045.If particle Reynolds number is less than 100, shield stress varies on varies of Reynolds number. This condition is for uniform sized and shape particles and homogenous on the bed [7, 31, 32]. During the analysis of sediment mixture, it is found that shape of the grain, orientation, exposure toward the bed, some bump on the bed and pocket geometry these all factors much influence the shield stress [33, 34].

If critical shield stress is constant in Equation 8 then smaller particles will move due to high mobility compared with large particles. This phenomenon also can see in Mountains River at steeper slopes. But many studies say that particles mobility higher than what get from shield stress Equation 8. It is due to friction angle and exposure of the particle. To calculate the shield stress at incipient motion in bulk mixtures of sediment through a single grain size called median grain size (D_{50}). D_{50} has been used in Equations 8 and 11 [32, 35].

In many research, for bedload transport model critical shield stress is assumed to be not varying with slope because it was largely unexplored that what the tendency of critical shield stress with slope. At steeper slopes, due to an increase of relative roughness critical shield stress value also increases and as a result mobility of the particle is reduced. k_s is the roughness length scale of the bed and h is the depth of flow in Equation 12 [36-38].

$$\text{Relative roughness} = \frac{k_s}{h} \tag{12}$$

In steady uniform flow, for a given total bed shear value, flow depth decreases when slope increases. Depth averaged flow velocity depends upon the relative roughness but local flow velocity depends upon the Z/k_s value. Where Z is the vertical height above the sediment bed level [39].

Further some past studies and after taking the flume and field published data show critical shield stress is dependent on the slope shown in Figure 6. Here critical shield stress includes wall drag, morphological and bed stress

without portioning of the individual [40, 41]. Most of the data has been collected for the particle Reynolds number is greater than 100. Particle Reynolds number less 100 gave a false relationship with a slope so avoided. Data in Figure 6 is such that it takes a regime where τ_c^* has a constant ranging from 0.03 to 0.06.There is a trend in Figure 6 that shows a relationship between τ_c^* and slope .This is the best fit line for good correlation with data [42, 43, 92]. Equation of best fit straight line for good R^2 value is given below in Equation 13.

$$\tau_c^* = 0.15S^{0.25} \tag{13}$$

Both data set having similar magnitude and trend for slope dependency on critical shield stress. But according to the study there is a lack of data for slope less than 0.001 and greater than 0.01 and τ_c^* the value falls between 0.03 and 0.06.

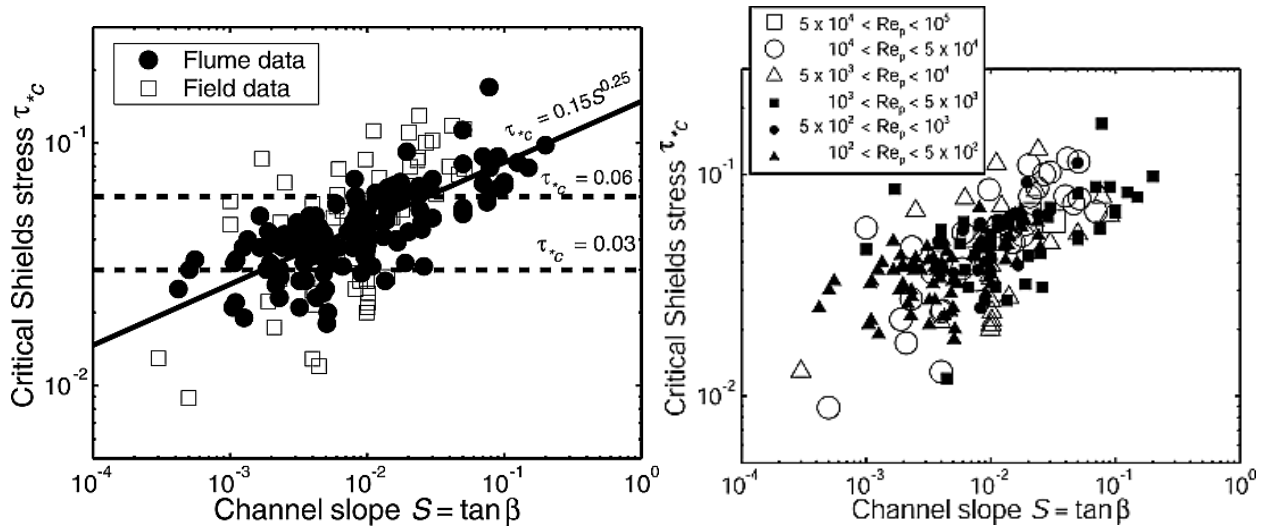

Figure 6. Slope dependency of critical shield stress [29] (a) The Compilation of flume data and field data separately; (b) The Compilation of flume data and field data with ranges of Reynolds Number

Now to understand the study of slope dependency upon critical shield stress, published studies have been reviewed based on the force balance model. This model gives you a real understanding based on the sort of equations involved in force balance [44, 45, 94].

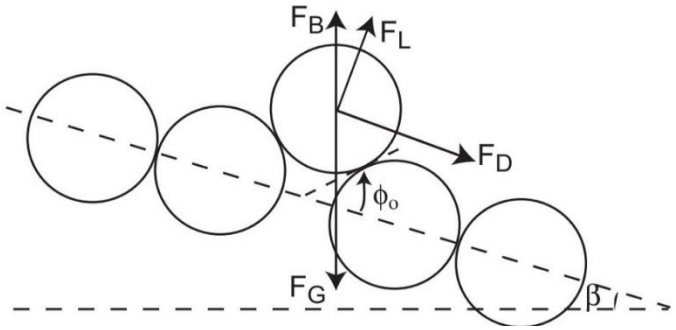

Figure 7. Modified force balance on particle including fluid forces, buoyant force and gravity force [29]

F_B, F_L, F_D are buoyant force, lift force and, drag force respectively in Figure 7 and acting to move the particle. Now force balance equation parallel to streambed to the given initial particle movement will be as follows:

$$F_D + (F_G + F_B)\sin\beta = [(F_G - F_B)\cos\beta - F_L]\tan\varphi_0 \tag{14}$$

$$F_D = \frac{1}{2}C_D\rho u^2 A \tag{15}$$

$$F_L = \frac{1}{2}C_L\rho u^2 A \tag{16}$$

$$F_B = \rho g V_1 \tag{17}$$

$$F_G = \rho_s g V_2 \tag{18}$$

φ_0 is the frictional angle between the particle and β is the inclination bed (S=tanβ);

ρ_s is the sediment particle density and ρ is fluid density;

C_D and C_L are the coefficient due to drag and lift respectively;

V_1 is submerged volume of particle and V_2 is volume of the sediment particle;

A is the area of the cross section of the particle perpendicular to the direction of flow and exposed to flow.

After putting the value of Equations 15 to 18 in Equation 14 and rearranging in terms of critical shield stress and get Equation 19.

$$\tau_{cg}^{*} = \frac{u_*^2}{rgD} = \frac{2}{C_D}\frac{u_*^2}{u^2}\cos\beta\left(\frac{tan\,\varphi_0 - \tan\beta}{1+\left(\frac{F_L}{F_D}\right)tan\,\varphi_0}\right).\left[\frac{V_2}{AD}\,\frac{1}{r}\left(\frac{\rho_s}{\rho}-\frac{V_1}{V_2}\right)\right] \quad (19)$$

Total bed stress will be due to channel wall drag, bed morphology, stream bed stress. Due to roughness in the channel, stress will be spent through these wall drag, bed morphology, and bed stress [46]. This individual stress is part of form drag and viscous shear stress. Bed morphology is also called morphological drag. Total bed stress is also called total driving stress at stream bed [47]. Two equations are written below to find total bed stress (Equations 20 and 21).

$$\tau_T = \tau_g + \tau_m + \tau_w \quad (20)$$

$$\tau_T = \rho g h \sin\beta \quad (21)$$

After combining Equations 19 to 21 with Equation 8, total critical shield stress is found and formed equation will cover total stress and low slope (S=tanβ). See in Equation 22;

$$\tau_{cT}^{*} = \frac{hS}{rD} = \frac{2}{C_D}\frac{u_*^2}{u^2}\left(\frac{\tau_T}{\tau_g+\tau_m+\tau_w}\right)\left(\frac{tan\,\varphi_0 - tan\,\beta}{1+\left(\frac{F_L}{F_D}\right)tan\,\varphi_0}\right)\left[\frac{V_2}{AD}\,\frac{1}{r}\left(\frac{\rho_s}{\rho}-\frac{V_1}{V_2}\right)\right] \quad (22)$$

The above equation 3.15 is the equation of total shield stress with slope dependency but in this equation when slope angle increases τ_{cT}^{*} value decreases means mobility of the particle increases. This is just the opposite of concerned analysis because according to flume and natural stream studies, the graph of best line fit in which increasing slope is producing an increase in critical shield stress. So as a conclusion for a given diameter of the particle D at least one of the variables in Equation 22 depends upon the channel slop or flow depth h.

In Equation 22 there are many variables involved to give slope dependency upon individual variable like wall drag, bed morphology, friction angle, emergence of the grain, Entrainment of the air, Average flow velocity, Fluctuation due to turbulent flow. After all total shield stress will have slope dependency according to behavior of the variables with respect to flow depth or slope.

This paper reviews slope dependency upon individual variable and they are described below:

I. Drag due to wall (τ_w): This is the drag or stress spent through the bank of channel. If any rectangular channel is considered then bed and wall of the channel are equally rough. This wall drag is very much important for small width to depth ratio (aspect ratio is small) according to Equation 23:

$$\tau_w = \left(\frac{2h}{w}\right)\tau_g \quad (23)$$

$$\tau_{cTR}^{*} = \frac{RS}{rD} = \frac{2}{C_D}\frac{u_*^2}{u^2}\left(\frac{\tau_T}{\tau_T-\tau_m}\right)\left(\frac{tan\,\varphi_0 - tan\,\beta}{1+\left(\frac{F_L}{F_D}\right)tan\,\varphi_0}\right)\left[\frac{V_2}{AD}\,\frac{1}{r}\left(\frac{\rho_s}{\rho}-\frac{V_1}{V_2}\right)\right] \quad (24)$$

τ_{cTR}^{*} is critical shield stress due to drag wall. This formulation is based on the same roughness at bed and wall. This formula is not used for the triangular channel because there is a wide difference between the roughness of the wall and bed. Now neglecting all wall correction, the critical shield stress will perform slope dependency. If increase the slope (neglecting wall corrections) then width to depth ratio will decrease or the roughness of channel bank related to bed roughness increases. Therefore width to depth ratio provides an inversely relation with slope in case of the natural stream. In Figure 6 partial or more correction on the wall (roughness correction) has been applied because Field measurement has more wall correction than experimental measurement [48, 49]. Application of all possible wall corrections give more accurate results over critical shield stress.

II. Morphological drag (τ_m) and friction angle (φ_0): It is convenient to observe that if bottom slope increases then drag also increases due to morphological changes. There are two types of drag in which form drag contribution will be more than viscous drag. This form drag is spent on morphological structure [50]. A flow separation will take place at rear portion of the structure. If there is an increase in the slope, form drag will increase means roughness increases.

The magnitude of morphological drag for turbulent flow depends upon the size of morphologic structure and square of the local time area- averaged velocity around the structural element. At steeper slope the value of τ_m increases and ultimately the value of τ_{cT}^* in Equation 22. Besides morphological changes, there will be changes in the angle of internal friction accordingly. It may be due to differences in shape and orientation of the sediments [51]. Some study says if morphological or form drag increases means particles come in the stable condition, the value of φ_0 will increase. But sand and gravel (cohesionless soil) can have a smoothing effect. It can reduce the friction angle and finally τ_{cT}^*.It means sand may be more movable at low slope. Hence there is no finding of any proper increase with a slope like morphological change. It provides undesirable results during flume experiments. Hence for flume experiments, frictional angle is independent on slope, is considered to make analysis easy but this paper also reviewed for friction angle [52-54]. Variations in friction angles occur due to variations in shapes, orientations, and sorting of the sediments. These variations can be seen in a natural stream. For experimental analysis, a graph is plotted in Figure 14(b).

The effect of morphology is approximately negligible for an experiment made on the flume. At steeper slope very negligible change in structure due to morphology. Anyone can surprise that even natural stream data doesn't more depend upon the morphological structure at a steeper slope. In Figure 6(a) for natural stream data more of the data is above the regression line for slope greater than 0.02. It means after this slope value there is a slight effect of frictional angles and morphological changes with slope.

III. Emergence of the particle from the flow*:* When a particle emerges from the flow then the area of cross-section and buoyant force both reduces. Mobility of the grain reduces at steeper slope when particle emerges from the flow. This effect can be shown in Equation 22 by writing one term $\left[\frac{V_2}{AD}\frac{1}{r}\left(\frac{\rho_s}{\rho}-\frac{V_1}{V_2}\right)\right]$. In this term area decreases, this whole term increases, and finally this term gives an impact on total critical shield stress. But the above term cannot fully explain the trends on slope dependent. Because shield criterion has been reported for slope less than 0.01 and grain was fully submerged as shown in the Figure 6(a) but other author study shows at threshold point, sediment grains are not emergent from the flow for slope less than 0.1 [43].

IV. Air Entrainment: When air enters in the water system then water air mixture reduces its own density. It decreases the movement of a particle at an increasing slope. It can also affect the mean flow velocity and bulk friction factor. Mean flow velocity will increase due to reduction of drag force and buoyant force. This Reduction in drag force plus buoyant force will increase the value of τ_{cT}^* at steeper slope. Aeration cannot completely explain the slope dependency of the total critical shield parameter, as substantial aeration exists mostly in steep slopes [55].

V. Drag coefficient (C_D) and lift coefficient (C_L): Through several studies in the past, it has been found C_D depends on the particle Reynolds number (Re_P).But τ_c^* is independent of high-value particle Reynolds number. For an isolated spherical particles with Reynolds number more than 10^5, C_D value decreases from 0.5 to 0.3 which is a kind of drag crisis. Some researchers showed that for increasing value of Reynolds number in between (100-10^5) decrease the value τ_c^*. Figure 6(b) shows that incipient motion based on particle Reynolds number [56, 57].

Very little work done for lift coefficient (low particle submergence with steep stream).Some researchers showed that fluctuations of pressure within a porous bed also can cause lift force on the emergent particle [56, 58].

VI. Average flow velocity: The remaining term in Equation 22 means velocity term u/u^* also a part of total critical shield stress. Average flow velocity is the function of (k_s/h) and local flow velocity is function (z/k_s) shown in Figure 8**,** where z is the height above river bed. Local flow velocity is independent of (k_s/h) and h (depth of the flow).Hence it is independent of the slope of bed for a given value average bed shear stress [39, 46, 91].

$$\frac{\bar{u}(z)}{u^*}=\frac{1}{k}\ln\left(\frac{z}{z_o}\right) \tag{25}$$

Where k is the von Karman's constant =0.4 and $z_o=k_s/30$ for hydraulically rough flow.

For a given value of k_s and τ_{cT}^* any increase in flow depth will not give any changes in flow velocity at any location on bed of particles. It is necessary to explain the mixing length in roughness zone [59, 60]. Mixing is governed by wakes. These wakes is formed back portion of the particle. The mixing length can be defined through Equation 26.

$$L=\alpha_1 k_s \tag{26}$$

$$\frac{\bar{u}}{u^*}=\frac{z}{\alpha_1 k_s}\left(1-\left(\frac{z}{2k_s}\frac{k_s}{h}\right)\right) \tag{27}$$

α_1 = Constant of proportionality less than unity.

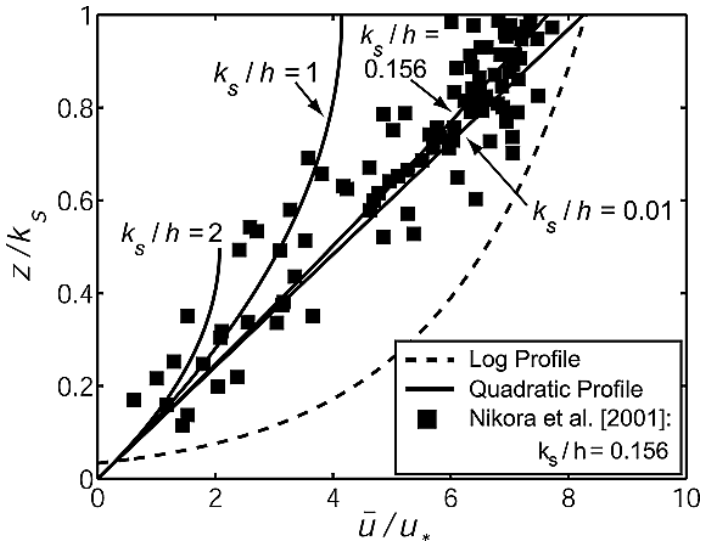

Figure 8. Velocity prediction for log profile in Equation 25 and quadratic profile in Equation 27 [29]

VII. Fluctuation due to turbulence: A Local velocity component is not only relevant for sediment's mobility but turbulent fluctuation is also important especially in a steep bed stream. And due to turbulence profiles are not logarithmic. The intensity of turbulence fluctuation is denoted by (σ_u/u^*) where σ_u is the root mean square velocity of the stream. Intensity varies with height above the bed and has peak value near bed surface for hydraulically smooth flow & top of roughened particle for hydraulically rough flow. The Peak value of σ_u/u^* is called the universal constant ($\sigma_{u,max}/u^*$). Some study says universal constant has the value between 2.2to 2.8 but others say universal constant is not constant. It varies with relative submergence (h/k_s) or relative roughness [4, 47, 61]. It is shown in Figure 9.

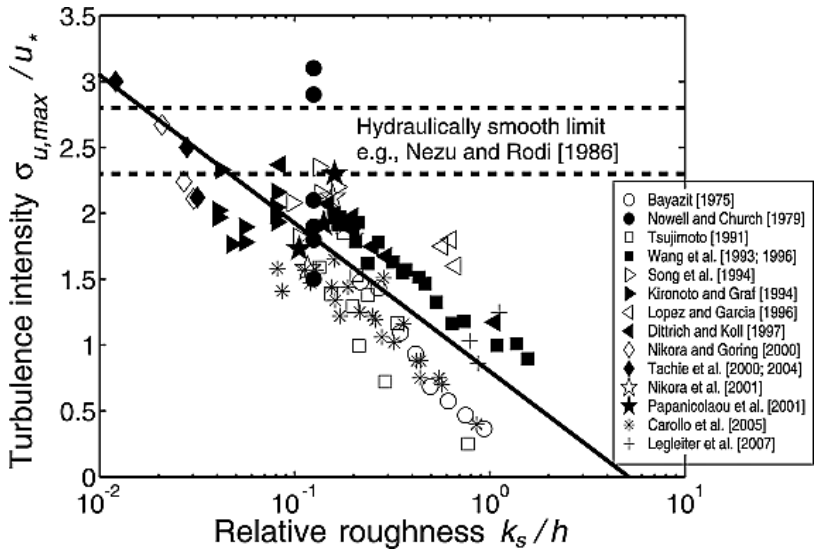

Figure 9. A relationship between turbulence intensity with relative roughness [29]

Authors formed a relation in which average flow velocity is a function of relative roughness then it is clear $\sigma_{u,max}/u^*$ will be function of average flow velocity. See in Equation 28;

$$\frac{\sigma_{u,max}}{u*} = \alpha_2 \frac{U}{u*} \tag{28}$$

Where α_2 is the proportionality constant between average flow velocity and peak near the bed intensity of turbulence [29]. In solid line is best line to fit the data with $\alpha_2 = 0.2$ for Equation 28.

3. Experimental Study Over Critical Shield's Stress

Shields experiment and diagram given by the shield for the specific type of particles (granite, amber, coal, barite) shown in Figure 4(a). Now studies of many researchers for different size range of gravel and sand particle (cohesionless alluvial soil), angle of internal friction, a slope angle, homogeneity and heterogeneity of river bed,

different velocity profiles, different submergence factor, different roughness factor etc. are discussed below [43, 51, 62-70]. For cohesive soil, resisting forces are cohesive forces between different particles and submerged weight. Due to cohesion tractive shield stress value becomes more than noncohesive soil. For cohesive soil, critical shear stress depends upon consolidation pressure and clay content. For cohesive soil, lumps of particles move as a single unit. From different studies a satisfactory Shields theory exists for only non-cohesive soil [93, 95].

Here in Table 1 have shown laboratory data and field data of angle of internal friction, slope angle, relative submergence, particle Reynolds number and critical shear stress respectively. As per table is the most recent one is laboratory data and this data has been taken as a point of interest to compare with past [65]. They studied on particle size 6-35.5 mm. Summary of the sediment has been provided in Table 2.

Table 1. Previous studies on entrainment condition [65]

Author(s)	φ (φ = f (d)) (°)	sin α (%)	h/d (R/d)(–)	R∗ (–)	θc (–)
Meyer-Peter and Müller (1948) (laboratory data) [63]	36	0.49–1.05	9.7–18.1	575–686	0.037–0.050
Neill (1967a, 1967b) (laboratory data) [62, 70]	35	0.85–2.7	4.9–14.3	596–1987	0.029–0.041
Kališ (1970) (laboratory data) [98]	45	5.9–9.2	0.94–1.47	10,889–17,963	0.032–0.059
Fenton and Abbott (1977) – series B (laboratory data) [74]	(35.3;38)	0.52–1.90	5.45–7.50	405–820	0.080–0.267
Fenton and Abbott (1977) – series C (laboratory data) [74]	35.3	0.5–1.6	2.8–4.4	1690–3280	0.009–0.012
Mizuyama (1977) (laboratory data) [88]	52.4;45	1–20	0.6–8.5	463–3558	0.047–0.099
Bathurst and Simons (1979) (laboratory data) [96]	35	2–8	1.5–5.3	881–6198	0.090–0.193
Cao (1985) (laboratory data) [97]	35	1–9	1.2–8.6	3008–9567	0.053–0.088
Bathurst et al. (1987) (laboratory data) [98]	35;40.5;40	0.5–9	1.3–11.9	1059–11,296	0.036–0.099
Graf and Suszka (1987) (laboratory data) [77]	35;40.5	0.5–2.5	4.0–13.4	929–3816	0.034–0.063
Suszka (1991) (laboratory data) [99]	35	0.5–2.5	4.1–13.5	1086–3577	0.041–0.064
Papanicolaou (1997) (laboratory data) [100]	35.3	0.8–1.2	7.13–9.50	535–757	0.037–0.075
Shvidchenko and Pender (2000) (laboratory data) [43]	35	0.65–2.87	(3.6–11.9)	421–1514	0.045–0.068
Gregoretti (2000) (laboratory data) [66]	51.2;47.7	21–36	0.47–1.19	4616–8963	0.131–0.236
Dey and Raju (2002) (laboratory data) [67]	35	0.73–1.85	1.4–5.7	400–1977	0.026–0.097
Mueller et al. (2005) (field measurements) [64]	35	0.21–5.09	3.2–14.9	5582–96,865	0.011–0.134
Aristide Lenzi et al. (2006) (field measurements) [51]	41.5	13.6	1.6–3.8	28,684–95,349	0.037–0.406
Recking (2006) (laboratory data) [101]	35	5–9	2.20–3.14	409–1808	0.077–0.153
Roušar et al. (2016) (laboratory data) [65]	35.3;41.5	1–7.5	0.76–7.16	523–4519	0.035–0.054

Table 1. Sediment properties used by Roušar et al. (2016) (laboratory data) [65]

Fraction (mm)	a (mm)	b ≈ d (mm)	c (mm)	Co (–)	ρ_s (kg m^{-3})	φ (°)	n (–)	C_{Dab} (–)	k_t (m s^{-1})
6–8	11.7	8.1	5.7	0.59	2674	35.3	0.42	1.35	0.03
8–10	13.7	9.5	6	0.52	2611	39.5	0.4	0.91	0.036
10–16	19.5	14.6	9.9	0.58	2876	38.5	0.4	1.33	0.061
16–20	28.2	20.3	13.9	0.58	2567	39.9	0.45	1.36	0.082
20–25	34.3	25.3	16.8	0.57	2632	41.5	0.42	1.5	0.084
25–31.5	43	31.5	21.5	0.58	2684	38.8	0.42	1.33	0.098

Here fraction of the particle, length (a),width (b),grain diameter (d),thickness (c),density of grains (ρ_s), angle of repose (φ), porosity of sediment (n), drag coefficient (C_{Dab}) perpendicular to the largest sediment area (a, b), Corey shape factor (Co), Hydraulic conductivity for subsurface flow (k_t). Roušar et al. (2016) [65] were used 6 fractions of particles mentioned in Table 2. They used 100 grains of each fraction. The Average size of grain in each fraction is a, b, c. Corey shape factor depends upon a, b, c value. $C_o=c/(ab)^{1/2}$. Drag coefficient (C_{Dab}) was found from Equation 29. The flow in the pores are turbulent and k_t value in Table 2 derives from Equation 30. For a different fraction, different ranges of discharge were used and multiple number of measurements for each fraction shown in Table 3.

$$C_{Dab} = 4(\rho_s - \rho)gc/(3\rho w^2) \quad (29)$$

$$k_t = \bar{u}_x n/(\sin\alpha)^{1/2} \quad (30)$$

Table 2. Hydraulic parameters with number of measurements for each fraction [65]

Fraction (mm)	h (mm)	Q (l s^{-1})	Sinα (%)	h/d (-)	R* (-)	θ_c (-)	Number of measurements
6–8	30-58	7.9-19.8	1.0-2.0	3.70-7.16	523-603	0.038-0.050	6
8–10	19-62	5.0-23.5	1.0-3.5	1.95-6.25	699-823	0.036-0.049	8
10–16	23-72	7.3-32.9	1.5-4.0	1.68-4.97	1286-1504	0.036-0.047	10
16–20	21-85	4.5-32.9	1.5-6.0	1.05-4.18	1976-2327	0.041-0.054	11
20–25	32-77	9.8-36.0	2.5-5.0	1.23-3.05	2899-3250	0.038-0.048	20
25–31.5	24-74	8.1-36.0	3.0-7.5	0.76-2.35	3658-4519	0.035-0.050	14

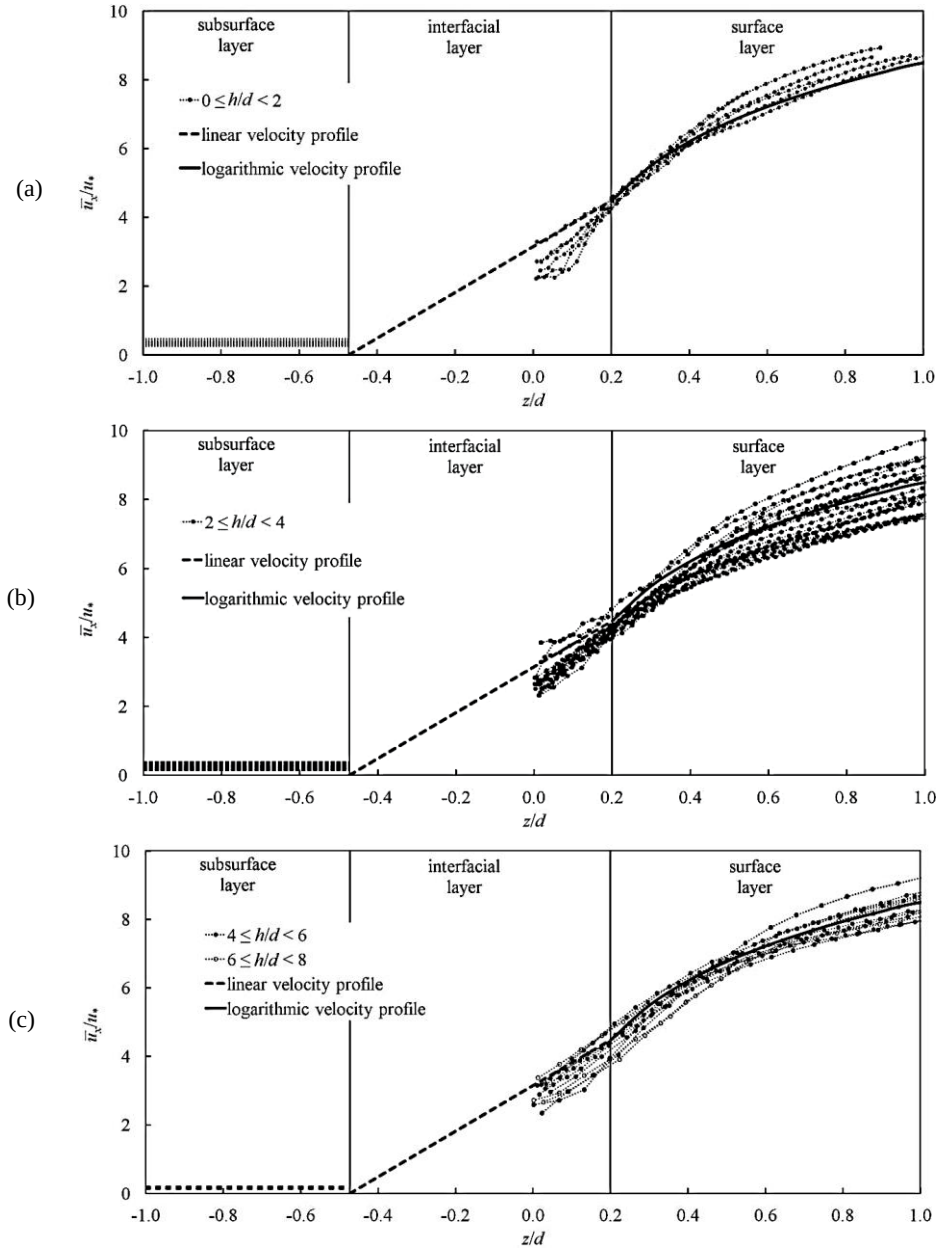

Figure 10. Velocity profile at different layer of bed [65] (a) 0≤h/d≤2; (b) 2≤h/d≤4; (c) 4≤h/d≤6 and 6≤h/d≤8

Roušar et al. (2016) [65] plotted a graph between time and area-averaged velocity ratio and relative height z/d. Figure 10 shows h/d (relative submergence) does not affect the velocity profile. This time-averaged velocity profile is also unaffected by (z/d)>0.2.The velocity profile of inferential layer is determined by linear extrapolation from observed value 0< (z/d) <0.2 to the value of velocity in subsurface layer and they agree with Pokrajac and Manes (2009) [71] measurements. In subsurface layer, velocity is approximately zero. Figure 10 also shows that the thickness of the grains is equal to the thickness of the inferential layer. Nikora et al. (2004) and Shimizu et al. (1990) [72, 73] also show interfacial values behave in same category. The boundary between interfacial and surface boundary lies in the range 0.2< (z/d) <0.4 but it is considered (z/d) =0.2 by Roušar et al. (2016).

(a)

(b)

(c)

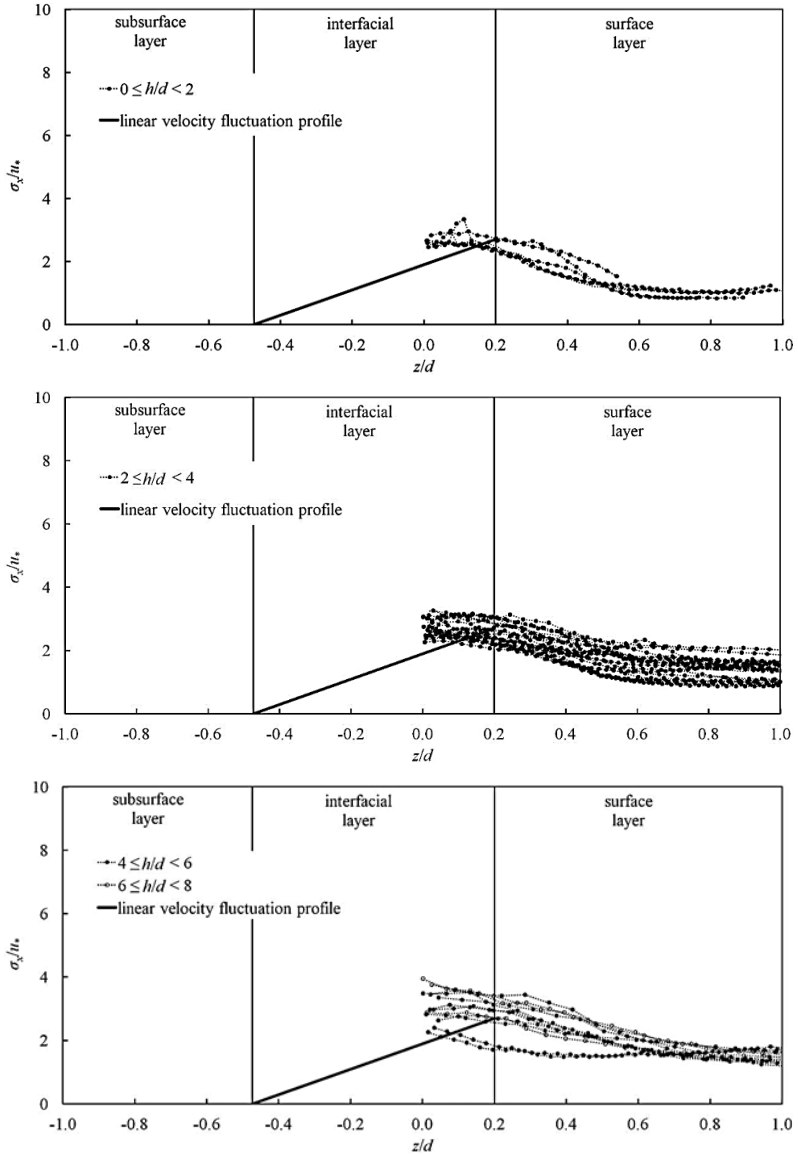

Figure 11. Normalized standard deviation (σx/u*) at different layers of bed (z/d) [65] (a) 0≤h/d≤2; (b) 2≤h/d≤4; (c) 4≤h/d≤6 and 6≤h/d≤8

(σ_x/u_*) is normalized standard deviation in x-direction of velocity profile where σ_x is the standard deviation of velocity in x- direction (u_x). Figure 11 shows the maximum value of σ_x/u_* is between (1.7 to 3.5) for all measured studies. Roušar et al. (2016) graph shows this value 2.6 and exists at (z/d)=0.2. This value has a good validation with Pokrajac and Manes [71].

(a)

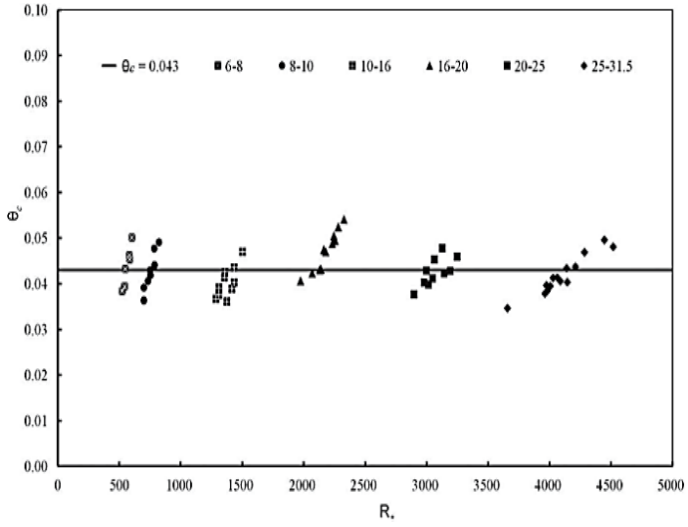

(b)

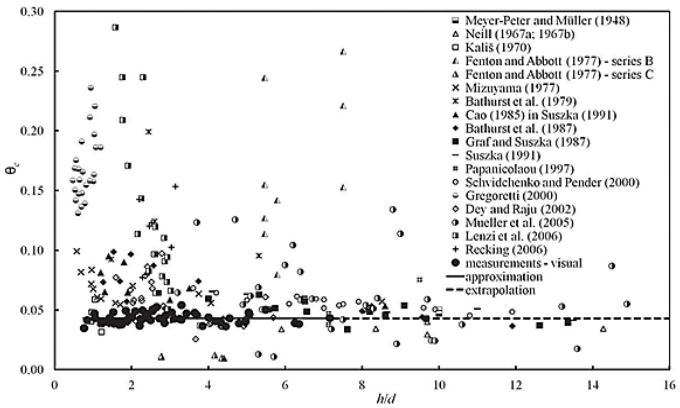

Figure 12. Relationship between particle Reynolds number and relative submergance over critical shear stress [65] (a) Reynolds number; (b) studies from all authors for relative submergence (dotted line shows extrapolation and solid line approximation).

Here Figure 12(a) shows that higher and higher values of Raynolds number don't affect the critical shear stress because velocity profiles don't change. Roušar et al. (2016) showed that the mean value of critical shear stress for the used grains will be approximately 0.043. Figure 12(b) shows that studies done by all the authors provide the same plot.Incipient motion of the particle is critical on lesser values of h/d depends upon the position of grains with bed.In other words it depends upon exposure of grains to the flow, the relative degree of submergence of the sediment particles, and self aeration. Roušar et al. (2016) did not take the data for the self aerated flow. Kališ (1970) [69] mentioned the effect of relative submergence for self-areation of flow and enlights the uncertainty involved in finding the bed levels. Figure 12(b) shows the relative submergence impact over critical shear stress based on non-zero value of dimensionless volume bedload discharge $q^* = q_b/(\Delta g d^3)^{1/2}$. This was given by Bathurst et al. and Suszka where q_b is a specific volume bedload discharge. However,different selected value of q^* gives different plots so these data were not used.

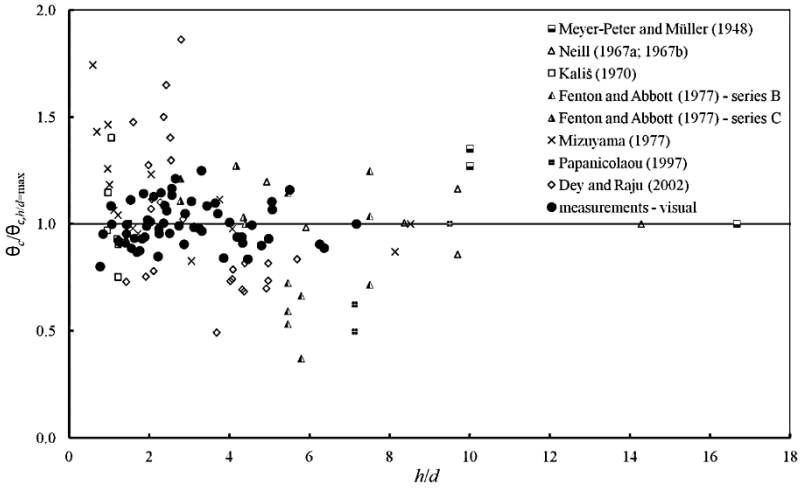

Figure 13. Relationship between relative submergence and absolute critical condition for grain incipient motion [65]

Figure 13 shows the relationship between critical shear stress and relative submergance at absolute level fullfilling the condition that is planner bed with roughness through grains should be homogeneous and submerged grains.The data of Dey and Neill (1967a, b), Raju (2002), Kališ (1970), Fenton and Abbott (1977), Mizuyama (1977) [62, 67, 69, 70, 74, 88] based upon these consideration. Figure 13 also shows the value of crtical shild stress with repect to shield stress value at the largest submergance means $\theta_c/\theta_{c,h/d=max}$ is function of h/d.

(a)

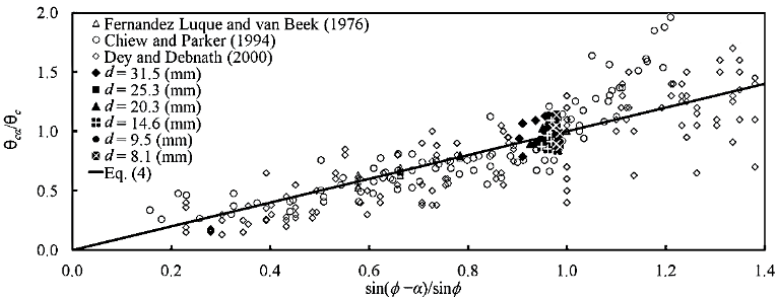

(b)

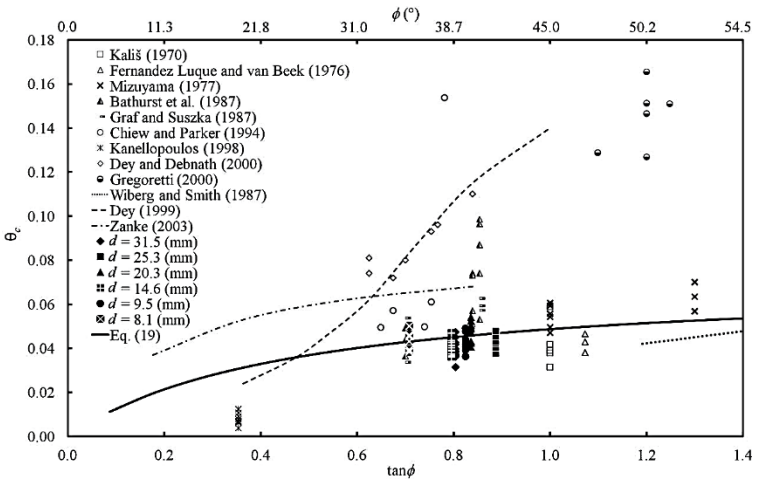

Figure 1. (a) Effect of longitudinal bed slope on critical shear stress (b) Effect of angle of repose on critical shear stress [65]

The effect of sinα on θ_c is given by following Equation 31;

$$\theta_c = \theta_{c\alpha}\left(\frac{\sin\phi}{\sin\phi - \alpha}\right) \tag{31}$$

Where θ_c is critical shear stress at horizontal plane, $\theta_{c\alpha}$ is the critical shear stress at an angle α

According to laboratory data (Figure 14 (a)) from different studies [74-76] confirm that slope angle has an affect on threshold motion of particle. And measured data provides a satisfactory results with Equation 29.

Figure 14(b) shows effect of angle of repose on critical shear stress. Many authors obtained θ_c values satisfying $(h/d)\geq 1$ and $R_*\geq 100$ [46, 69, 76, 77, 88]. Roušar et al. (2016) experiments shows $0.03 < \theta_c < 0.06$. In most of the data it shows relationship with an increase in value of $\tan\phi$ with increase of θ_c. It is shown in Equation 32.

$$\theta c = \frac{tan\ \varphi}{6.5\ +\ 14\ tan\ \varphi} \tag{32}$$

In Figure 14(b) solid line follows the Equation 30.

4. Remarks and Discussion

This paper reviewed the analysis of threshold motion of particle given by many authors through laboratory and field data to measure the critical tractive stress.To find the shear stress by Shield's approach is implicit log-log plot approach.Due to implicity, it makes many applications complex and inconvenient.So there is more required to make the explicit formulation of shields parameter [78]. Guo (2002) [79] provided a logarthamic matching method critical shield stress can be directly determined with fluid and sediment properties. Yalin and da salva [80, 81] proposed how the critical parameter varies with particle size. He replaced the particle Raynolds number with the material number. This type of theoretical approach also incorporate all phenomenon such as lift force, gravity force, drag force, fluctuation due to turbulence and these ultimately fulfills the sliding, rolling and lifting. Many researchers uses sliding as the main mechanism and gave less importance to roll and very few for lifting but all are equally important based on force balance over the particles [78, 82]. Iwagaki (1956), Ikeda (1982) and Coleman (1967) model [25, 83, 84] is based on sliding concept. They didn't talk about turbulence and particle placement on the bed. Dey (2014) [16] worked on the rolling concept for incipient motion. He took the effect of magnus force also but no turbulence.Sundborg modified the hjulstorm diagram with taking consideration of cohesion and further it was improved for consolidated and unconsolidated soil. But here different shortcomings arise and there is the requirement to lead for more research .First is there was no well-defined exposure and protrusion level used.So some correction is required to make more sense. Very little analysis has been done on lifting so more study is required to improve the suspended load transport mechanism. Bravo et al. (2014) [82] presented a mathematical modelling means the use of discrete element method (numerical micro dynamics model) and here saltation mode and suspended mode of moving particle implies more detailed flow detailing and this may be large scale dynamics so there is a large improvement in the model.Furthur discrete element method is valid for a large number of particles simulation. He didn't talk about the effect of the numerical microdynamics model on cohesive soil or mixed- grained soil. At the last, these are more important for future improvement because due to various dynamics involved with river and coastal areas and accuracy of erosion threshold is much essential for various scouring and erosion process like general,contraction,local scouring.

Very small work has been done on slope effect dependency over lift coefficient which is a variable for total critical shield stress. At steeper slope with low submergence value of particle analysis of lift coefficient is much needed. Schmeeckle et al. (2007) and Nelson et al. (2001) [56, 85] did a measurement on lift coefficient and found lift force can not scale with the difference in velocity of particle which was inconsistent with flow based on Bernoulli principle.The calculation of lift is very important when grains are not emerging from the flow.Pressure fluctuations from the bed also give a lift force hence for calculation point of view study becomes more important [86, 87]. There is a lack of data and lift force theory so it makes difficult in the force balance model.Proper investigation and research in the future are required with high accuracy data and relevant theory.

5. Conclusions

Experimental studies, done by many researchers on critical shield parameter and dependable variables (Bottom channel slope, Raynolds number, relative roughness, turbulence intensity, flow velocity, angle of internal friction etc.), show well explanation for sediment transportation conditions based on tractive stress analysis.This paper reviewed the channel slope dependency on critical shield stress, wherein most of tha data are based on total stress.These data are a compilation of both flume and field data separately by different researchers.They showed the best fit line with an r-square value of 0.41. These data have been filtered so that particle Raynolds number is greater 100. With summarized analysis researchers assumed that critical shield stress value lies between 0.03 to 0.06 for gravel bed shown in Figure 6(a). For more good results some researchers showed that critical shield stress decreases with increasing particle Raynolds number (constant slope) and plotted a graph in Figure 6(b) to notice dependency.As per the concluding analysis of this paper, lift coefficient measurement is also important during slope dependency analysis,especially in steeper streams and low particle submergence.It is difficult to add lift into force balance equation owning to lack of theory and data.

Further, This paper reviewed the laboratory and field measurements of cohesionless sediments.After analysis of sediment properties and hydraulic parameters with the number of measurements for each fraction of sediments,graphical relations have been presented.There is almost zero velocity or no velocity profile at subsurface layer but interfacial and surface layer possess linear and logarithmic velocity profile respectively at the value of relative submergence between zero and eight.This is shown in Figure 10. Linear velocity fluctuation profiles also have been shown in Figure 11 at $0 \leq z/d \leq 8$. Normalized standard deviation is the flagship to check the profiles at different layers of bed and its maximum value lies between 1.7 to 3.5 at somewhere boundary of the interfacial and surface layer.The velocity profiles do not change with particle Raynolds number and this conclusion is verified by Figure 12(a),where a relationship between critical shield parameter and particle Raynolds number is shown.The effect of relative submergence (position of grains to bed) has little effect on critical shield parameter shown by different researchers in Figure 12(b). In brief, paper reviewed there is neglect effect of particle Raynolds number and realtive submergance over critical shield parameter.

The effect of angle of repose $\tan\phi$ over critical shield parameter has been reviewed in Figure 14(b) and thoroughly explained for different sizes of grains.Only experiments confirm the character of this relationship because drag ,lift and proportionality coefficient have different values for different lab measurements and material but some researchers provide an equation after numerical simulations shown in Equation 32 and it agrees with the values obtained from the experiment.

6. Declarations

6.1. Author Contributions

All authors contributed equally to write this manuscript and all authors have read and agreed to the published version of the manuscript.

6.2. Data Availability Statement

No new data were created or analyzed in this study. Data sharing is not applicable to this article.

6.3. Funding

The authors received no financial support for the research, authorship, and/or publication of this article.

6.4. Conflicts of Interest

The authors declare no conflict of interest.

7. References

[1] Sutherland, Alex J. “Proposed Mechanism for Sediment Entrainment by Turbulent Flows.” Journal of Geophysical Research 72, no. 24 (December 15, 1967): 6183–6194. doi:10.1029/jz072i024p06183.

[2] Ninto, Y., and M. H. Garcia. “Experiments on Particle—turbulence Interactions in the Near–wall Region of an Open Channel Flow: Implications for Sediment Transport.” Journal of Fluid Mechanics 326 (November 10, 1996): 285–319. doi:10.1017/s0022112096008324.

[3] Simões, Francisco JM. "Shear velocity criterion for incipient motion of sediment." Water Science and Engineering 7, no. 2 (2014): 183-193. doi:10.3882/j.issn.1674-2370.2014.02.006.

[4] Zanke, U. C. E. "On the influence of turbulence on the initiation of sediment motion." International Journal of Sediment Research 18, no. 1 (2003): 17-31.

[5] Einstein, Hans Albert, and El-Sayed Ahmed El-Samni. “Hydrodynamic Forces on a Rough Wall.” Reviews of Modern Physics 21, no. 3 (July 1, 1949): 520–524. doi:10.1103/revmodphys.21.520.

[6] Southard J. “Introduction to Fluid Motions, Sediment Transport, and Current-Generated Sedimentary Structures.” Massachusetts Inst Technol MIT OpenCourseWare, (2006):260–284.

[7] Miller, M. C., I. N. McCave, and P. D. Komar. “Threshold of Sediment Motion under Unidirectional Currents.” Sedimentology 24, no. 4 (August 1977): 507–527. doi:10.1111/j.1365-3091.1977.tb00136.x.

[8] Yang, Yang, Shu Gao, Ya Ping Wang, Jianjun Jia, Jilian Xiong, and Liang Zhou. “Revisiting the Problem of Sediment Motion Threshold.” Continental Shelf Research 187 (October 2019): 103960. doi:10.1016/j.csr.2019.103960.

[9] Chepil, W. S. “The Use of Spheres to Measure Lift and Drag on Wind-Eroded Soil Grains.” Soil Science Society of America Journal 25, no. 5 (September 1961): 343–345. doi:10.2136/sssaj1961.03615995002500050011x.

[10] Balachandar, Ram, and Faruk Bhuiyan. “Higher-Order Moments of Velocity Fluctuations in an Open-Channel Flow with Large Bottom Roughness.” Journal of Hydraulic Engineering 133, no. 1 (January 2007): 77–87. doi:10.1061/(asce)0733-9429(2007)133:1(77).

[11] Sundborg, Åke. “The River Klarälven a Study of Fluvial Processes.” Geografiska Annaler 38, no. 2–3 (August 1956): 125–316. doi:10.1080/20014422.1956.11880887.

[12] Dey, Subhasish, and Sk Zeeshan Ali. “Review Article: Advances in Modeling of Bed Particle Entrainment Sheared by Turbulent Flow.” Physics of Fluids 30, no. 6 (June 2018): 061301. doi:10.1063/1.5030458.

[13] García, Marcelo H. "Sediment Transport and Morphodynamics." In Sedimentation engineering: Processes, measurements, modeling, and practice, (2008): 21-163.

[14] Valyrakis, Manousos. "Initiation of particle movement in turbulent open channel flow." PhD diss., Virginia Tech, United States, (2011).

[15] Dey, Subhasish, Sankar Sarkar, and Luca Solari. “Near-Bed Turbulence Characteristics at the Entrainment Threshold of Sediment Beds.” Journal of Hydraulic Engineering 137, no. 9 (September 2011): 945–958. doi:10.1061/(asce)hy.1943-7900.0000396.

[16] Dey, Subhasish. “Sediment Threshold.” Fluvial Hydrodynamics (2014): 189–259. doi:10.1007/978-3-642-19062-9_4.

[17] Buffington, John M., and David R. Montgomery. “A Systematic Analysis of Eight Decades of Incipient Motion Studies, with Special Reference to Gravel-Bedded Rivers.” Water Resources Research 33, no. 8 (August 1997): 1993–2029. doi:10.1029/96wr03190..

[18] Iversen, J.D., J.B. Pollack, R. Greeley, and B.R. White. “Saltation Threshold on Mars: The Effect of Interparticle Force, Surface Roughness, and Low Atmospheric Density.” Icarus 29, no. 3 (November 1976): 381–393. doi:10.1016/0019-1035(76)90140-8.

[19] Iversen, James D., Ronald Greeley, John R. Marshall, and James B. Pollack. “Aeolian Saltation Threshold: The Effect of Density Ratio.” Sedimentology 34, no. 4 (August 1987): 699–706. doi:10.1111/j.1365-3091.1987.tb00795.x.

[20] Ward, Bruce D. “Relative Density Effects on Incipient Bed Movement.” Water Resources Research 5, no. 5 (October 1969): 1090–1096. doi:10.1029/wr005i005p01090.

[21] Ali, Sk Zeeshan, and Subhasish Dey. “Hydrodynamics of Sediment Threshold.” Physics of Fluids 28, no. 7 (July 2016): 075103. doi:10.1063/1.4955103.

[22] Salim, Sarik, Charitha Pattiaratchi, Rafael O. Tinoco, and Ravindra Jayaratne. "Sediment Resuspension Due to Near‐Bed Turbulent Effects: A Deep Sea Case Study on the Northwest Continental Slope of Western Australia." Journal of Geophysical Research: Oceans 123, no. 10 (October 2018): 7102–7119. doi:10.1029/2018jc013819.

[23] C. M. White "The Equilibrium of Grains on the Bed of a Stream." Proceedings of the Royal Society of London. Series A. Mathematical and Physical Sciences 174, no. 958 (February 21, 1940): 322–338. doi:10.1098/rspa.1940.0023.

[24] M. Kurihara. "On the critical tractive force." Research Institute for Hydraulic Engineering, Japan 4, (1948).

[25] Iwagaki, Yuichi. "(I) Hydrodynamical Study on Critical Tractive Force." Transactions of the Japan Society of Civil Engineers 1956, no. 41 (1956): 1–21. doi:10.2208/jscej1949.1956.41_1.

[26] Reichardt, H. "Vollständige Darstellung Der Turbulenten Geschwindigkeitsverteilung in Glatten Leitungen." ZAMM - Zeitschrift Für Angewandte Mathematik Und Mechanik 31, no. 7 (1951): 208–219. doi:10.1002/zamm.19510310704.

[27] Wiberg, Patricia L., and J. Dungan Smith. "Calculations of the Critical Shear Stress for Motion of Uniform and Heterogeneous Sediments." Water Resources Research 23, no. 8 (August 1987): 1471–1480. doi:10.1029/wr023i008p01471.

[28] Morsi, S. A., and A. J. Alexander. "An Investigation of Particle Trajectories in Two-Phase Flow Systems." Journal of Fluid Mechanics 55, no. 02 (September 1972): 193-208. doi:10.1017/s0022112072001806.

[29] Lamb, Michael P., William E. Dietrich, and Jeremy G. Venditti. "Is the Critical Shields Stress for Incipient Sediment Motion Dependent on Channel-Bed Slope?" Journal of Geophysical Research 113, no. F2 (May 1, 2008). doi:10.1029/2007jf000831.

[30] Armanini, Aronne, and Carlo Gregoretti. "Incipient Sediment Motion at High Slopes in Uniform Flow Condition." Water Resources Research 41, no. 12 (December 2005): 1-8. doi:10.1029/2005wr004001.

[31] Tipper, J.C. "The Equilibrium and Entrainment of a Sediment Grain." Sedimentary Geology 64, no. 1–3 (August 1989): 167–174. doi:10.1016/0037-0738(89)90090-0.

[32] Bridge, John S., and Sean J. Bennett. "A Model for the Entrainment and Transport of Sediment Grains of Mixed Sizes, Shapes, and Densities." Water Resources Research 28, no. 2 (February 1992): 337–363. doi:10.1029/91wr02570.

[33] Komar, Paul D., and Paul A. Carling. "Grain Sorting in Gravel-Bed Streams and the Choice of Particle Sizes for Flow-Competence Evaluations." Sedimentology 38, no. 3 (June 1991): 489–502. doi:10.1111/j.1365-3091.1991.tb00363.x.

[34] Kirchner, James W., William E. Dietrich, Fujiko Iseya, and Hiroshi Ikeda. "The Variability of Critical Shear Stress, Friction Angle, and Grain Protrusion in Water-Worked Sediments." Sedimentology 37, no. 4 (August 1990): 647–672. doi:10.1111/j.1365-3091.1990.tb00627.x.

[35] Ferguson, Robert I. "Emergence of abrupt gravel to sand transitions along rivers through sorting processes." Geology 31, no. 2 (2003): 159-162. doi:10.1130/0091-7613(2003)031<0159:EOAGTS>2.0.CO;2.

[36] Lisle, T. E. "Overview: channel morphology and sediment transport in steepland streams." Erosion and Sedimentation in the Pacific Rim (Proceedings of the Corvallis Symposium, August 1987). International Association of Hydrological Sciences Pub. No. 165, (1987): 287-297.

[37] Aminoroayaie Yamini, O., S. Hooman Mousavi, M. R. Kavianpour, and Azin Movahedi. "Numerical Modeling of Sediment Scouring Phenomenon Around the Offshore Wind Turbine Pile in Marine Environment." Environmental Earth Sciences 77, no. 23 (November 24, 2018). doi:10.1007/s12665-018-7967-4.

[38] Buffington, John M., and David R. Montgomery. "Effects of Hydraulic Roughness on Surface Textures of Gravel-Bed Rivers." Water Resources Research 35, no. 11 (November 1999): 3507–3521. doi:10.1029/1999wr900138.

[39] Gordon RJ. "Boundary Layer Theory." AIChEMI Modul Instr Ser C Series C: TRANSPORT, Volume 7: Calculation and Measurement Techniques for Momentum, Energy and Mass Transfer, (1983): 23–27.

[40] Wilcock, Peter R., and Brian W. McArdell. "Surface-Based Fractional Transport Rates: Mobilization Thresholds and Partial Transport of a Sand-Gravel Sediment." Water Resources Research 29, no. 4 (April 1993): 1297–1312. doi:10.1029/92wr02748.

[41] Komar, Paul D. "Selective Gravel Entrainment and the Empirical Evaluation of Flow Competence." Sedimentology 34, no. 6 (December 1987): 1165–1176. doi:10.1111/j.1365-3091.1987.tb00599.x.

[42] Hammond, F. D. C., A. D. Heathershaw, and D. N. Langhorne. "A comparison between Shields' threshold criterion and the movement of loosely packed gravel in a tidal channel." Sedimentology 31, no. 1 (1984): 51-62. doi:10.1111/j.1365-3091.1984.tb00722.x.

[43] Shvidchenko, Andrey B., and Gareth Pender. "Flume Study of the Effect of Relative Depth on the Incipient Motion of Coarse Uniform Sediments." Water Resources Research 36, no. 2 (February 2000): 619–628. doi:10.1029/1999wr900312.

[44] Wilcock, Peter R. "Methods for Estimating the Critical Shear Stress of Individual Fractions in Mixed-Size Sediment." Water Resources Research 24, no. 7 (July 1988): 1127–1135. doi:10.1029/wr024i007p01127.

[45] Tsujimoto, Tetsuro. "Bed-Load Transport in Steep Channels." Lecture Notes in Earth Sciences (1991): 89–102. doi:10.1007/bfb0011185.

[46] Chiew, Yee-Meng, and Gary Parker. "Incipient Sediment Motion on Non-Horizontal Slopes." Journal of Hydraulic Research 32, no. 5 (September 1994): 649–660. doi:10.1080/00221689409498706.

[47] McLean, S. R., and V. I. Nikora. "Characteristics of Turbulent Unidirectional Flow over Rough Beds: Double-Averaging Perspective with Particular Focus on Sand Dunes and Gravel Beds." Water Resources Research 42, no. 10 (October 2006): 1-19. doi:10.1029/2005wr004708.

[48] Vanoni, Vito A., and Norman H. Brooks. "Laboratory studies of the roughness and suspended load of alluvial streams." No. 11. US Army Engineer Division, Missouri River, (1957).

[49] Parker, Gary, Peter R. Wilcock, Chris Paola, William E. Dietrich, and John Pitlick. "Physical Basis for Quasi-Universal Relations Describing Bankfull Hydraulic Geometry of Single-Thread Gravel Bed Rivers." Journal of Geophysical Research 112, no. F4 (November 2, 2007). doi:10.1029/2006jf000549.

[50] Mueller, Erich R. "Morphologically Based Model of Bed Load Transport Capacity in a Headwater Stream." Journal of Geophysical Research 110, no. F2 (2005): 1-14. doi:10.1029/2003jf000117.

[51] Aristide Lenzi, Mario, Luca Mao, and Francesco Comiti. "When Does Bedload Transport Begin in Steep Boulder-Bed Streams?" Hydrological Processes 20, no. 16 (2006): 3517–3533. doi:10.1002/hyp.6168.

[52] Braudrick, Christian A., and Gordon E. Grant. "When Do Logs Move in Rivers?" Water Resources Research 36, no. 2 (February 2000): 571–583. doi:10.1029/1999wr900290.

[53] Yager, E. M., J. W. Kirchner, and W. E. Dietrich. "Calculating Bed Load Transport in Steep Boulder Bed Channels." Water Resources Research 43, no. 7 (July 2007). doi:10.1029/2006wr005432.

[54] Wilcox, Andrew C., Jonathan M. Nelson, and Ellen E. Wohl. "Flow Resistance Dynamics in Step-Pool Channels: 2. Partitioning Between Grain, Spill, and Woody Debris Resistance." Water Resources Research 42, no. 5 (May 2006). doi:10.1029/2005wr004278.

[55] Chanson, H. "Drag Reduction in Skimming Flow on Stepped Spillways by Aeration." Journal of Hydraulic Research 42, no. 3 (January 2004): 316–322. doi:10.1080/00221686.2004.9728397.

[56] Schmeeckle, Mark W., Jonathan M. Nelson, and Ronald L. Shreve. "Forces on Stationary Particles in Near-Bed Turbulent Flows." Journal of Geophysical Research 112, no. F2 (April 11, 2007). doi:10.1029/2006jf000536.

[57] Lawrence, D. S. L. "Hydraulic Resistance in Overland Flow during Partial and Marginal Surface Inundation: Experimental Observations and Modeling." Water Resources Research 36, no. 8 (August 2000): 2381–2393. doi:10.1029/2000wr900095.

[58] Schwendel, Arved C., Russell G. Death, and Ian C. Fuller. "The Assessment of Shear Stress and Bed Stability in Stream Ecology." Freshwater Biology 55, no. 2 (February 2010): 261–281. doi:10.1111/j.1365-2427.2009.02293.x.

[59] Nikora, Vladimir, Derek Goring, Ian McEwan, and George Griffiths. "Spatially Averaged Open-Channel Flow over Rough Bed." Journal of Hydraulic Engineering 127, no. 2 (February 2001): 123–133. doi:10.1061/(asce)0733-9429(2001)127:2(123).

[60] Defina, Andrea, and Anna Chiara Bixio. "Mean Flow and Turbulence in Vegetated Open Channel Flow." Water Resources Research 41, no. 7 (July 2005). doi:10.1029/2004wr003475.

[61] Hofland, Bas, Jurjen A. Battjes, and Robert Booij. "Measurement of Fluctuating Pressures on Coarse Bed Material." Journal of Hydraulic Engineering 131, no. 9 (September 2005): 770–781. doi:10.1061/(asce)0733-9429(2005)131:9(770).

[62] Neill C.R. "Mean-velocity criterion for scour of coarse uniform bed-material." Twelfth Congress of the International Association for Hydraulic Research, Fort Collins: Colorado State University 3, (1967): 46–54.

[63] Meyer-Peter E, Müller R. "Formulas for Bed-Load Transport." Proceedings of the 2nd Meeting of the International Association of Hydraulic Research, IAHR, (1948):39–64.

[64] Mueller, Erich R., John Pitlick, and Jonathan M. Nelson. "Variation in the Reference Shields Stress for Bed Load Transport in Gravel-Bed Streams and Rivers." Water Resources Research 41, no. 4 (April 2005). doi:10.1029/2004wr003692.

[65] Roušar, Ladislav, Zbyněk Zachoval, and Pierre Julien. "Incipient Motion of Coarse Uniform Gravel." Journal of Hydraulic Research 54, no. 6 (August 16, 2016): 615–630. doi:10.1080/00221686.2016.1212286.

[66] Gregoretti, Carlo. "The Initiation of Debris Flow at High Slopes: Experimental Results." Journal of Hydraulic Research 38, no. 2 (March 2000): 83–88. doi:10.1080/00221680009498343.

[67] Dey, Subhasish, and Uddaraju V. Raju. "Incipient Motion of Gravel and Coal Beds." Sadhana 27, no. 5 (October 2002): 559–568. doi:10.1007/bf02703294.

[68] Asheghi, Reza, and Seyed Abbas Hosseini. "Prediction of Bed Load Sediments Using Different Artificial Neural Network Models." Frontiers of Structural and Civil Engineering 14, no. 2 (March 16, 2020): 374–386. doi:10.1007/s11709-019-0600-0.

[69] Kališ J. "Hydraulic research of boulder chutes." In Brno University of Technology, (1970).

[70] Neill CR. "Stability of coarse bed-material in open-channel flow." Res Counc Alberta, (1967).

[71] Pokrajac, Dubravka, and Costantino Manes. "Velocity Measurements of a Free-Surface Turbulent Flow Penetrating a Porous Medium Composed of Uniform-Size Spheres." Transport in Porous Media 78, no. 3 (February 7, 2009): 367–383. doi:10.1007/s11242-009-9339-8.

[72] Nikora, Vladimir, Katinka Koll, Ian McEwan, Stephen McLean, and Andreas Dittrich. "Velocity Distribution in the Roughness Layer of Rough-Bed Flows." Journal of Hydraulic Engineering 130, no. 10 (October 2004): 1036–1042. doi:10.1061/(asce)0733-9429(2004)130:10(1036).

[73] Shimizu, Yoshihiko, Tetsuro Tsujimoto, and Hiroji Nakagawa. "Experiment and macroscopic modelling of flow in highly permeable porous medium under free-surface flow." J. Hydrosci. Hydraul. Eng 8, no. 1 (1990): 69-78.

[74] Fenton, J. D. and J. E. Abbott "Initial Movement of Grains on a Stream Bed: The Effect of Relative Protrusion." Proceedings of the Royal Society of London. A. Mathematical and Physical Sciences 352, no. 1671 (February 4, 1977): 523–537. doi:10.1098/rspa.1977.0014.

[75] Dey, Subhasish, and Koustuv Debnath. "Influence of Streamwise Bed Slope on Sediment Threshold under Stream Flow." Journal of Irrigation and Drainage Engineering 126, no. 4 (July 2000): 255–263. doi:10.1061/(asce)0733-9437(2000)126:4(255).

[76] Fernandez Luque, R., and R. Van Beek. "Erosion And Transport Of Bed-Load Sediment." Journal of Hydraulic Research 14, no. 2 (April 1976): 127–144. doi:10.1080/00221687609499677.

[77] Graf, Walter Hans. "Sediment transport in steep channel." Jour. Hydroscience and Hydr. Eng., JSCE. 5, no. 1 (1987): 11-26.

[78] Cao, Zhixian, Gareth Pender, and Jian Meng. "Explicit Formulation of the Shields Diagram for Incipient Motion of Sediment." Journal of Hydraulic Engineering 132, no. 10 (October 2006): 1097–1099. doi:10.1061/(asce)0733-9429(2006)132:10(1097).

[79] Guo, Junke. "Logarithmic Matching and Its Applications in Computational Hydraulics and Sediment Transport." Journal of Hydraulic Research 40, no. 5 (September 2002): 555–565. doi:10.1080/00221680209499900.

[80] Yalin MS. "Mechanics of sediment transport." 2nd ed. University of Brighten, Oxford, (1977).

[81] Yalin, M. S. and da Silva AMF. "Fluvial Processes." IAHR International Association of Hydraulic Engineering, and Research, Delft, The Netherlands, (2001).

[82] Bravo, R., P. Ortiz, and J.L. Pérez-Aparicio. "Incipient Sediment Transport for Non-Cohesive Landforms by the Discrete Element Method (DEM)." Applied Mathematical Modelling 38, no. 4 (February 2014): 1326–1337. doi:10.1016/j.apm.2013.08.010.

[83] Ikeda, Syunsuke. "Incipient Motion of Sand Particles on Side Slopes." Journal of the Hydraulics Division 108, no. 1 (January 1982): 95–114. doi:10.1061/jyceaj.0005812.

[84] Coleman, Neil L. "A theoretical and experimental study of drag and lift forces acting on a sphere resting on a hypothetical streambed." (1967).

[85] Nelson, Jonathan M., Mark W. Schmeeckle, and Ronald L. Shreve. "Turbulence and particle entrainment." Gravel Bed Rivers V (2001): 221-248.

[86] Parker, Gary, and Marcelo H. Garcia, eds. "River, Coastal and Estuarine Morphodynamics" Proceedings of the 4th IAHR Symposium on River, Coastal and Estuarine Morphodynamics, London, Taylor and Francis, First Edition, (September 29, 2005): 65-69. doi:10.1201/9781439833896.

[87] Vollmer, Stefan, and Maarten G. Kleinhans. "Predicting Incipient Motion, Including the Effect of Turbulent Pressure Fluctuations in the Bed." Water Resources Research 43, no. 5 (May 2007). doi:10.1029/2006wr004919.

[88] Mizuyama, T. "Bedload transport in steep channels" (PhD dissertation), Kyoto University, Kyoto, (1977).

[89] Vanoni, Vito A., ed. "Sedimentation Engineering" American Society of Civil Engineers, Manuals and Reports on Engineering Practice 54 (March 29, 2006). doi:10.1061/9780784408230.

[90] Ahmad, Muhammad, Usman Ghani, Naveed Anjum, Ghufran Ahmed Pasha, Muhammad Kaleem Ullah, and Afzal Ahmed. "Investigating the Flow Hydrodynamics in a Compound Channel with Layered Vegetated Floodplains." Civil Engineering Journal 6, no. 5 (May 1, 2020): 860–876. doi:10.28991/cej-2020-03091513.

[91] Sun, Zhilin, Haolei Zheng, Dan Xu, Chunhong Hu, and Chaofan Zhang. "Vertical Concentration Profile of Nonuniform Sediment." International Journal of Sediment Research 36, no. 1 (February 2021): 120–126. doi:10.1016/j.ijsrc.2020.06.008.

[92] Unal, Necati. “Shear Stress-Based Analysis of Sediment Incipient Deposition in Rigid Boundary Open Channels.” Water 10, no. 10 (October 9, 2018): 1399. doi:10.3390/w10101399.

[93] Singh, Umesh K., Z. Ahmad, Ashish Kumar, and Manish Pandey. “Incipient Motion for Gravel Particles in Cohesionless Sediment Mixtures.” Iranian Journal of Science and Technology, Transactions of Civil Engineering 43, no. 2 (July 30, 2018): 253–262. doi:10.1007/s40996-018-0136-x.

[94] Carrillo, Veronica, John Petrie, Luis Timbe, Esteban Pacheco, Washington Astudillo, Carlos Padilla, and Felipe Cisneros. “Validation of an Experimental Procedure to Determine Bedload Transport Rates in Steep Channels with Coarse Sediment.” Water 13, no. 5 (March 2, 2021): 672. doi:10.3390/w13050672.

[95] Phillips, C. B., and D. J. Jerolmack. “Bankfull Transport Capacity and the Threshold of Motion in Coarse‐Grained Rivers.” Water Resources Research 55, no. 12 (December 2019): 11316–11330. doi:10.1029/2019wr025455.

[96] Bathurst, J. C., Li, R. M., & Simons, D. B. “Hydraulics of mountain rivers.” Fort Collins, CO: Colorado State University, (1979).

[97] Cao, H. H. “Resistance hydraulique d’un lit de gravier mobile a pente raide: etude experimentale.”, Thesis. EPFL (1985). doi: 10.5075/epfl-thesis-589

[98] Bathurst, J. C., Graf, W. H., Cao, H. H. “Bed load discharge equations for steep mountain rivers.” Sediment transport in gravel-bed rivers (1987):453-491.

[99] Suszka, Lechostaw. “Modification of Transport Rate Formula for Steep Channels.” Lecture Notes in Earth Sciences (1991): 59–70. doi:10.1007/bfb0011182.

[100] Papanicolaou, Athanasios N. "The role of turbulence on the initiation of sediment motion." PhD diss., Virginia Tech, United States, (1997).

[101] Recking, Alain. "An experimental study of grain sorting effects on bedload." Institut National des Sciences Appliquees de Lyon, Lyon, France, (2006).